

# Implications of IUGR-Related Geometric Heart Changes on the ECG and Electrophysiology: an In Silico Perspective

Freddy L Bueno-Palomeque<sup>1,2,3</sup>, Ernesto Zacur<sup>4</sup>, Esther Pueyo<sup>1,2</sup>, Fàtima Crispi<sup>5</sup>, Pablo Laguna<sup>1,2</sup>, Ana Mincholé<sup>1,2</sup>

<sup>1</sup> BSICoS Group, I3A, IIS Aragón, Universidad de Zaragoza, Zaragoza, Spain

<sup>2</sup> CIBER en Bioingeniería, Biomateriales y Nanomedicina (CIBER-BBN), Zaragoza, Spain

<sup>3</sup> GIHEA, Universidad Politécnica Salesiana, Cuenca, Ecuador

<sup>4</sup> Corify Care SL, Madrid, Spain

<sup>5</sup> BCNatal - Barcelona Center for Maternal-Fetal and Neonatal Medicine, Hospital Sant Joan de Déu and Hospital Clínic, University of Barcelona, Barcelona, Spain

## Abstract

*This study aimed to simulate the geometric changes resulting from intrauterine growth restriction (IUGR) in a realistic biventricular heart model and assess their impact on cardiac electrophysiology. Geometric alterations were based on echocardiography measurements from IUGR patients. The model exhibited a reduction in left ventricle sphericity index and an increase in left ventricular wall thickness. Results showed a significant prolongation of the QRS complex duration and an increase in R-wave magnitude when compared to control geometry, consistent with clinical findings. However, a modest increase in the  $T_{pe}$  interval, which aligns with clinical observations, is observed, while the QT interval shows a prolongation that contradicts clinical results. These findings suggest that while the simulated geometric changes reproduce certain clinical observations, others are not reproduced suggesting additional factors, such as changes in electrical activation and/or ionic remodeling influencing cardiac electrophysiology in IUGR, to be tested in future investigations.*

## 1. Introduction

An unfavorable intrauterine environment leads to the development of fetal intrauterine growth restriction (IUGR) and causes the cardiac muscle to adapt to the restricted conditions. IUGR affects 7-10% of pregnancies, with a significantly higher incidence in developing and underdeveloped countries compared to developed countries [1]. Cardiac remodeling induced by IUGR includes changes in cardiac geometry, such as a reduction in the sphericity index (SpI) (apex-to-base length ( $\mathcal{L}$ ) over basal diameter ( $\phi$ ),  $\text{SpI} = \mathcal{L}/\phi$ ) as reported by [2]. Additionally, there is an

increase in the ventricular wall thickness, or width, ( $\mathcal{W}$ ), predominantly affecting the left ventricle [3]. Together, these changes contribute to a more globular heart shape. Although cardiac remodeling may be compensated for in the first few months of life [4], evidence suggests that the sequels of IUGR can persist through childhood, adolescence, and even into adulthood [5], and its presence has been associated with cardiac diseases.

The remodeling induced by IUGR results in changes in the electrophysiological behavior of the cardiac muscle, causing variations in the angles of depolarization and repolarization, as measured by vectorcardiography (VCG) in preadolescents and adults [5, 6]. Besides, simulations on computational models have shown changes in depolarization and repolarization angles in VCG due to alterations in the SpI. However, the magnitude and direction of these changes vary across different angular projections [7].

Geometric alterations have been shown to affect electrical activation as evidenced by changes in the duration of the depolarization and repolarization phases in ECG data when comparing preadolescents with IUGR and controls [8]. However, it is not yet clear how a wider left ventricular  $\mathcal{W}$  and a shorter  $\mathcal{L}$  affect electrophysiological properties.

A prolonged QRS duration ( $\text{QRS}_d$ ) is a parameter associated with anatomical and functional cardiac abnormalities. This parameter is considered a predictor of congestive heart failure [9], incident atrial fibrillation [10], and death. In the repolarization phase, prolonged durations of the QT interval and the T-peak to T-end interval ( $T_{pe}$ ) have been identified as predictors of ventricular arrhythmias in severe cardiac conditions [11]. Additionally, the  $T_{pe}/QT$  ratio is considered an index of arrhythmogenesis [12].

The changes in the SpI, sequelae of IUGR, have been modeled *in silico*, under the hypothesis that an increase in the left ventricular  $\mathcal{W}$  would affect the T-wave morphol-

ogy, influencing the  $T_{pe}$  interval. However, in [8], no significant change in  $T_{pe}$ , a reduction of 1 ms in the  $QT$  interval, and an increase of 1 ms in the  $QRS_d$  were found.

Given the minimal changes observed in the T-wave and QRS parameters in simulations with just a reduced SpI, it was proposed to evaluate the impact of increasing the left ventricular width  $\mathcal{W}$ . In this context, the objective of this study was to not only reduce the SpI but also increase the left ventricular width  $\mathcal{W}$  *in silico*, simulating the geometric remodeling resulting from IUGR, to understand its impact on the  $QRS_d$  and the  $T_{pe}$  and  $QT$  intervals, which are markers associated with ventricular arrhythmias.

## 2. Materials and methods

For the development of this study, we started with a realistic biventricular heart model and its torso [13]. The mesh of the control model ( $\mathcal{C}$ ) consisted of 332,396 nodes and 1,977,117 elements. To generate the globular model ( $\mathcal{G}$ ), we began with the control model and altered its SpI based on data measured in subjects with IUGR [2]. For the globular anatomy, both ventricular  $\mathcal{W}$  were increased by 40% while keeping the endocardial dimensions, followed by a 9% shortening in the longitudinal direction. The geometric changes are summarized in Figure 1. Once the globular model was developed, it was remeshed (357,308 nodes and 2,144,025 elements). Both models utilized tetrahedral elements. Three beats were simulated, with a stimulus triggered every 1000 ms, having an amplitude of 200 mA and a duration of 0.5 ms.

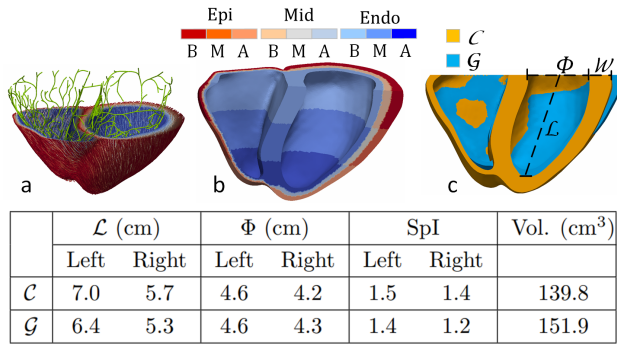


Figure 1. a) Fiber architecture and Purkinje network, b) transmural and apico-basal heterogeneities, and c)  $\mathcal{C}$  and  $\mathcal{G}$  models with  $\mathcal{L}$ ,  $\Phi$ , SpI,  $\mathcal{W}$  and volume representations.

For the activation and electrophysiological propagation in the  $\mathcal{C}$  model, a fiber architecture was incorporated using a rule-based method [14] and a Purkinje network based on a fractal design [15] (Figure 1.a). For the  $\mathcal{G}$  model, the same network used in the  $\mathcal{C}$  model was adapted to the endocardial surface of the ventricles. The ventricular walls were divided into 30% endocardium, 30% mid-myocardium, and 40% epicardium. Additionally, the

model was segmented into three sections along the apex-to-base direction (B, M, A: base, middle, and apex respectively), with the conductance  $G_{Ks}$  reduced progressively from 0% at the apex, to 49% in the middle, and 96% at the base (Fig. 1.b).

With the incorporation of the torso, a pseudo-ECG (pECG) was calculated with its 12 leads. The pECG was delineated, identifying the beginning and end of the QRS complex, and the peak and end of the T-wave, using an automatic delineator based on the Wavelet transform [16]. A single-lead delineator was used, adding a multilead rule to compute the mentioned parameters. Subsequently, a spatial transformation based on principal component analysis was performed, generating a new independent lead. A new lead (PCA<sub>QRS</sub> lead) was created using the QRS signal segment as the learning data set for the spatial transformation parameters and another new lead (PCA<sub>T</sub> lead) using the T-wave signal segment. The new leads were delineated again to identify the fiducial points: the peak of the R-wave, the beginning and end of the QRS complex were measured over lead PCA<sub>QRS</sub>, the peak of the T-wave, and its end over lead PCA<sub>T</sub> (Figure 2).

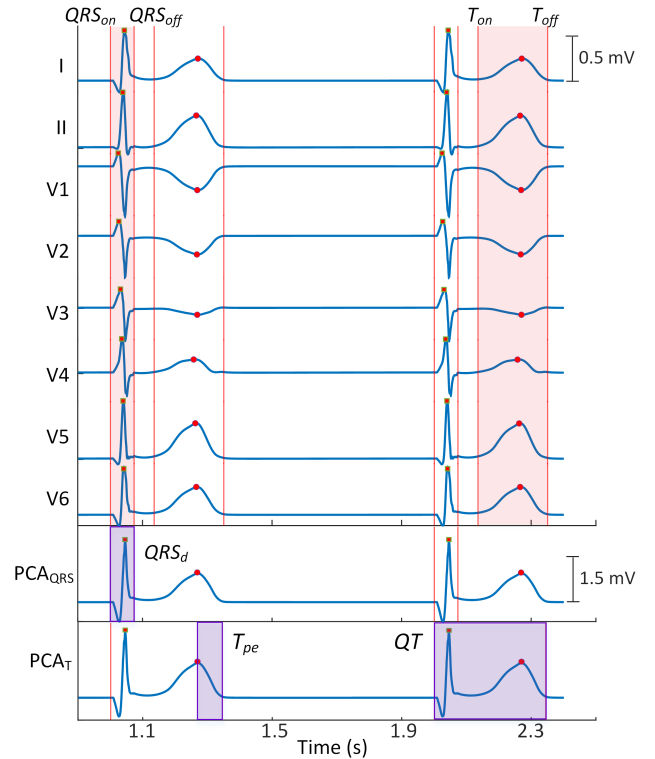


Figure 2. The independent 8 pECG leads from the  $\mathcal{C}$  model with marks on QRS and T-wave onset and end with red long lines, R and T peaks with red squares and circles respectively. Similarly, PCA<sub>QRS</sub> and PCA<sub>T</sub> with definitions of  $QRS_d$ ,  $T_{pe}$ , and  $QT$  shaded in purple.

	ECG data			Simulation	
	Control (n = 60)	IUGR (n = 33)	<i>p</i> -value	$\mathcal{C}$	$\mathcal{G}$
QRS <sub>d</sub> (s)	0.083 (0.074 - 0.089)	0.087 (0.081 - 0.090)	0.039	0.064	0.076
T <sub>pe,c</sub> (s)	0.076 (0.074 - 0.081)	0.078 (0.076 - 0.083)	0.030	0.076	0.079
QT <sub>c</sub> (s)	0.391 (0.376 - 0.406)	0.389 (0.381 - 0.399)	0.703	0.340	0.344
T <sub>pe,c</sub> /QT <sub>c</sub>	0.196 (0.188 - 0.207)	0.202 (0.196 - 0.212)	0.020	0.223	0.229
QRS <sub>a</sub> (mV)	2.98 (2.42 - 3.57)	3.11 (2.38 - 3.64)	0.553	1.86	2.04
T <sub>a</sub> (mV)	0.82 (0.63 - 0.99)	0.77 (0.56 - 0.89)	0.318	1.21	1.33

Table 1. Median and interquartile range and *p*-value for intervals QRS<sub>d</sub>, T<sub>pe,c</sub>, QT<sub>c</sub>, and T<sub>pe,c</sub>/QT<sub>c</sub>, and amplitudes QRS<sub>a</sub> and T<sub>a</sub>, measurements on the control and IUGR subjects groups [8]. The two most right columns show the results obtained in the simulation of the  $\mathcal{C}$  and  $\mathcal{G}$  models.

The duration of the QRS complex, the T<sub>pe</sub> and QT intervals were then measured. Similarly, the amplitudes of the QRS complex (QRS<sub>a</sub>) and the T-wave (T<sub>a</sub>) were measured, over leads PCA<sub>QRS</sub> and PCA<sub>T</sub>, respectively.

### 3. Results

The delineation performed on the PCA<sub>QRS</sub> and PCA<sub>T</sub> leads is shown in Figure 3, for  $\mathcal{C}$  and  $\mathcal{G}$  models. The results of the interval and amplitude measurements are presented in Table 1, along with the results measured from clinical ECGs as presented in [8].

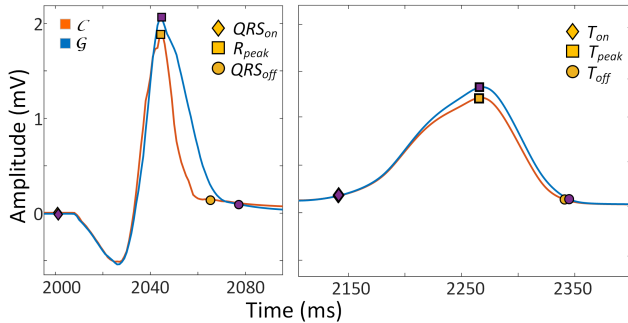


Figure 3. QRS complex and T-wave from the PCA<sub>QRS</sub> (left panel) and PCA<sub>T</sub> (right panel) leads on the  $\mathcal{C}$  and  $\mathcal{G}$  models. The marks show the onset, peak, and end of the QRS complex and T-wave.

The  $\mathcal{G}$  model exhibited a prolonged QRS<sub>d</sub> of 12 ms. The T<sub>pe</sub> interval showed an increase of 3 ms in the  $\mathcal{G}$  model. In the same model, the QT interval displayed an increase of 4 ms, and an increase of 0.006 in the T<sub>pe</sub>/QT ratio. Regarding amplitude, the QRS<sub>a</sub> showed a higher value in the  $\mathcal{G}$  model with 2.04 mV, and the T<sub>a</sub> also showed a higher value of 1.33 mV in this model.

### 4. Discussion

The present study focused on analyzing the changes in the duration of markers in the depolarization and repolar-

ization stages simulated in a realistic biventricular control heart model and a globular model representing the geometric change resulting from IUGR. The parameters that guided the geometric change in SpI were derived from echocardiographic measurements performed on IUGR patients and reported in [2,3]. The increase in thickness  $\mathcal{W}$  of the left ventricular wall was done using the relationship explained in the materials and methods section, with a greater increase at the ventricular base (Figure 1.c). The Purkinje network was adapted to the change in SpI and connected to the diminished endocardial tissue. This structural adaptation reduced the ventricular activation time, although the change was subtle and it was not perceptible in the pECG or reflected in the annotations on it (Figure 3).

The  $\mathcal{G}$  model reduced its left SpI by 8.6% and the right by 8.4%. When considering only the reduction in SpI in simulation, without  $\mathcal{W}$  modifications, this variation did not produce significant intervals or amplitudes changes as presented in [8]. However, an increase in  $\mathcal{W}$  of the ventricular wall has resulted in a significant change in QRS<sub>d</sub> from 64 ms to 76 ms, aligning with the clinical results shown in [8]. The geometric changes applied to the  $\mathcal{G}$  model, on the other hand, did not produce a large change in the T<sub>pe</sub> interval (an increase of 3 ms), although it is consistent with the clinical findings [8], where a significant difference in T<sub>pe,c</sub> was found (*p*-value = 0.030), with a median variation of 2 ms. In the QT interval, the simulation showed an increase of 4 ms, contrary to what was observed in clinical data, where there is a reduction of 2 ms. In the work presented by [8], the left ventricular  $\mathcal{W}$  was increased by 0.2 mm, while in the present study,  $\mathcal{W}$  was increased a maximum by 2.8 mm at the left ventricular base (Figure 1.c).

The increase in ventricular volume has resulted in a greater prolongation of the QRS<sub>d</sub> and an increase in the amplitude of the R-wave, QRS<sub>a</sub> (Figure 3), as measured in the PCA<sub>QRS</sub> lead. The variation in ventricular volume had a minimal effect on the duration of the T-wave; however, its impact on the amplitude, particularly in the maximum T<sub>a</sub> magnitude is more pronounced.

## 5. Conclusions

The results of this study have shown that simulating geometric heart changes resulting from IUGR generates outcomes consistent with those observed in clinical data. The increase in  $QRS_d$  (12 ms) has been amplified when the ventricular thickness is increased in the simulation. The increase in  $T_{pe}$  aligns with the clinical results, although the ventricular thickness increase has not significantly augmented this interval (2 ms). Regarding the  $QT$  interval, an increase of 4 ms has been observed, which is not in line with the clinical observations. The simulated geometric change resulting from IUGR is associated with the increase in  $QRS_d$ , whose prolongation is associated with heart failure and death. On the other hand, the impact of the heart geometric change on the T-wave and its characteristic points indicates poor alignment with observed clinical results, suggesting that there may be additional electrical activation modifications and ionic remodeling that have not been considered in the simulation.

## Acknowledgments

Funding was provided by: Ph.D. scholarship to L. Bueno from Fundación Carolina, Univ. de Zaragoza, and Univ. Politécnica Salesiana; projects PID2021-128972OA-I00, PID2022-140556OB-I00, CNS2022-135899, and TED2021-130459B-I00 from AEI, Spain; BSICoS group T39.23R from Aragón Government, and a personal fellowship RYC2019-027420-I to A. Mincholé.

## References

- [1] Sharma D, Shastri S, Sharma P. Intrauterine growth restriction: antenatal and postnatal aspects. *Clinical Medicine Insights Pediatrics* 2016;10:CMPed-S40070.
- [2] Sarvari SI, Rodríguez M, Nuñez-García M, Sitges M, Sepulveda-Martínez A, Camara O, Butakoff C, Gratacós E, Bijmens B, Crispi F. Persistence of cardiac remodeling in preadolescents with fetal growth restriction. *Circulation Cardiovascular Imaging* jan 2017;10(1). ISSN 1941-9651.
- [3] Cruz-Lemini M, Crispi F, Valenzuela-Alcaraz B, Figueras F, Gómez O, Sitges M, Bijmens B, Gratacós E. A fetal cardiovascular score to predict infant hypertension and arterial remodeling in intrauterine growth restriction. *American Journal of Obstetrics and Gynecology* 2014;210(6):552–e1.
- [4] Ross MG, Beall MH. Adult sequelae of intrauterine growth restriction. *Seminars in Perinatology* 2008;32:213–218. ISSN 01460005.
- [5] Ortigosa N, Rodríguez M, Bailón R, Sepulveda-Martínez A, Gratacós E, Crispi F, Laguna P. Intrauterine growth restriction induced ECG morphological differences measured in adulthood. *Computing in Cardiology* 2018;2018-Sept:3–6. ISSN 2325887X.
- [6] Ortigosa N, Rodríguez M, Bailón R, Sarvari SI, Sitges M, Gratacós E, Bijmens B, Crispi F, Laguna P. Heart morphology differences induced by intrauterine growth restriction and preterm birth measured on the ECG at preadolescent age. *J Electrocardiol* 2016;49(3):401–409. ISSN 15328430.
- [7] Bueno-Palomeque FL, Mountris KA, Ortigosa N, Bailón R, Bijmens B, Crispi F, Pueyo E, Mincholé A, Laguna P. QRS-T angles as markers for heart sphericity in subjects with intrauterine growth restriction: a simulation study. *IEEE Journal of Biomedical and Health Informatics* 2023;.
- [8] Bueno-Palomeque FL, Mountris KA, Ortigosa N, Bailón R, Bijmens B, Crispi F, Pueyo E, Mincholé A, Laguna P. Qrs width and t-peak to t-end interval are prolonged in preadolescents with severe intrauterine growth restriction at birth when compared to controls. In *2023 Computing in Cardiology (CinC)*, volume 50. 2023; 1–4.
- [9] Ilkhanoff L, Liu K, Ning H, Nazarian S, Bluemke DA, Soliman EZ, Lloyd-Jones DM. Association of qrs duration with left ventricular structure and function and risk of heart failure in middle-aged and older adults: The multi-ethnic study of atherosclerosis (mesa). *European Journal of Heart Failure* 11 2012;14:1285–1292. ISSN 13889842.
- [10] Aeschbacher S, O’Neal WT, Krisai P, Loehr L, Chen LY, Alonso A, Soliman EZ, Conen D. Relationship between qrs duration and incident atrial fibrillation. *International Journal of Cardiology* 9 2018;266:84–88. ISSN 0167-5273.
- [11] Yamaguchi M, Shimizu M, Ino H, Terai H, Uchiyama K, Kotaro O, Mabuchi T, Konno T, Kaneda T, Mabuchi H. T wave peak-to-end interval and QT dispersion in acquired long QT syndrome: A new index for arrhythmogenicity. *Clinical Science* 2003;105(6):671–676. ISSN 01435221.
- [12] Gupta P, Patel C, Patel H, Narayanaswamy S, Malhotra B, Green JT, Yan GX.  $T_{pe}/QT$  ratio as an index of arrhythmogenesis. *J Electrocardiol* 2008;41(6):567–574. ISSN 00220736.
- [13] Mincholé A, Zacur E, Ariga R, Grau V, Rodríguez B. MRI-based computational torso/biventricular multiscale models to investigate the impact of anatomical variability on the ECG QRS complex. *Frontiers in Physiology* 2019;10:1103.
- [14] Doste R, Soto-Iglesias D, Bernardino G, Alcaine A, Sebastian R, Giffard-Roisin S, Sermesant M, Berruezo A, Sanchez-Quintana D, Camara O. A rule-based method to model myocardial fiber orientation in cardiac biventricular geometries with outflow tracts. *International Journal for Numerical Methods in Biomedical Engineering* apr 2019; 35(4). ISSN 20407947.
- [15] Costabal FS, Hurtado DE, Kuhl E. Generating Purkinje networks in the human heart. *Journal of Biomechanics* 2016; 49(12):2455–2465.
- [16] Martínez JP, Almeida R, Olmos S, Rocha AP, Laguna P. A Wavelet-Based ECG Delineator Evaluation on Standard Databases. *IEEE Transactions on Biomedical Engineering* apr 2004;51(4):570–581. ISSN 00189294.

Address for correspondence:

Freddy L Bueno-Palomeque  
Universidad Politécnica Salesiana, Calle Vieja 12-30 and Elia Liut, 010102, Cuenca, Ecuador  
fbueno@ups.edu.ec